On the Phase Structure of the Micromaser System

Per Kristian Rekdal[1,*] and Bo-Sture Skagerstam[1,2,†]

[1]Department of Physics, The Norwegian University of Science and Technology, N-7034 Trondheim, Norway
[2]Theoretical Physics Division, CERN, CH-1211 Geneva 23, Switzerland

We investigate, in an exact manner, the phase structure of the micromaser system in terms of the physical parameters at hand like the atom cavity transit time τ, the atom-photon frequency detuning $\Delta\omega$, the number of thermal photons n_b and the probability a for a pump atom to be in its excited state. Phase diagrams are mapped out for various values of the physical parameters. At sufficiently large values of the detuning we find a "twinkling" mode of the micromaser system. A correlation length is used to study fluctuations close to the various phase transitions.

PACS numbers 32.80.-t, 42.50.-p, 42.50.Ct

There are few systems in physics which exhibit a rich struture of phase transitions that can be investigated under clean experimental conditions and which at the same time can be studied by exact theoretical methods. The micromaser system, which is a remarkable experimental realization of the idealized system of a two-level atom interacting with a second quantized single-mode electromagnetic field, provides us with such an example (for reviews and references see e.g. [1]).

Many features of the micromaser are of general interest. It can e.g. be argued that the micromaser system is a simple illustration of the conjectured topological origin of second-order phase transitions [2]. Various aspects of stochastic resonance can, furthermore, be studied in this system [3]. The micromaser also illustrates a feature of non-linear dynamical systems: turning on randomness may led to an increased signal to noise ratio [4].

In a typical realization of the micromaser, the pump atoms which enter the cavity are assumed to be prepared in an incoherent mixture, i.e. the density matrix ρ_A of the atoms is diagonal with diagonal matrix elements a and b such that $a+b=1$. In terms of the dimensionless atomic flux parameter $N = R/\gamma$, where R is the rate injected atoms and γ is the damping rate of the cavity, the stationary photon number probability distribution is then well known [5] and is given by

$$p_n = p_0 \prod_{m=1}^{n} \frac{n_b\, m + N a q_m}{(1+n_b)\, m + N b q_m} \quad . \tag{1}$$

Here $q_m \equiv q(m/N)$ and

$$q(x) = \frac{x}{x+\Delta^2}\ \sin^2\left(\theta\sqrt{x+\Delta^2}\,\right) \quad , \tag{2}$$

where we have defined the dimensionless detuning $\Delta = \Delta\omega/(2g\sqrt{N})$ and pump $\theta = g\tau\sqrt{N}$ parameters. Furthermore, g is the single photon Rabi frequency at zero detuning of the Jaynes-Cummings (JC) model [6]. The overall constant p_0 is determined by $\sum_{n=0}^{\infty} p_n = 1$.

The theory as developed in Refs. [5,7] suggests the existence of various phase transitions in the large N limit as the parameter θ is increased. A natural order parameter is then the average photon "density" $\langle x\rangle$, where $\langle\ \rangle$ denotes an average with respect to the distribution Eq. (1) and $x = n/N$. An exact treatment, in the large N limit, of the micromaser phases structure and the corresponding critical fluctuations in terms of a conventional correlation length has been given in Refs. [8]. Spontaneous jumps in $\langle n\rangle/N$ and large correlation lengths close to micromaser phase transitions have actually been observed experimentally [1,9]. Most of the theoretical and experimental studies have, however, been limited to the case $a = 1$ and $\Delta = 0$. It is the purpose of the present paper to study the phase structure of the micromaser system for general a and Δ using methods which are exact in the large N limit [8]. As will be argued below, several new intriguing physical properties of the micromaser system are then unfolded.

In order to obtain an appropriate expression for p_n which describes the various micromaser phases, we notice that the equilibrium distribution in Eq. (1) can be rewritten by using the Poisson summation technique [10]. The equilibrium distribution then takes the form

$$p(x) = p_0\sqrt{\frac{w(x)}{w(0)}}\ e^{-N\,V(x)} \quad , \tag{3}$$

where we have defined an effective potential $V(x) = \sum_{k=-\infty}^{\infty} V_k(x)$ and

$$V_k(x) = -\int_0^x d\nu\ \ln[\,w(\nu)\,]\,\cos(2\pi N k\nu) \quad , \tag{4}$$

$$w(x) = \frac{n_b\, x + a\, q(x)}{(1+n_b)\, x + b\, q(x)} \quad . \tag{5}$$

*email: perr@phys.ntnu.no
†email: boskag@phys.ntnu.no

In the large N limit Eq. (3) can be simplified by making use of a saddle-point approximation. The saddle-points are then determined by $V_0'(x) = 0$. If such non-trivial saddle-points exist we say that they describe maser phases. In a topological analysis of the second-order phase transitions [2] of the micromaser system, $V_0(x)$ will play the role of a Morse function.

If the only global minimum of $V_0(x)$ corresponds to $x = 0$, we expand the effective potential around the origin. The micromaser is then in a thermal phase and we obtain

$$p_n = p_0 \left(\frac{n_b + a\,\theta_{eff}^2}{1 + n_b + b\,\theta_{eff}^2} \right)^n \quad , \tag{6}$$

which is normalizable provided $\theta_{eff}^2\,(a-b) < 1$, where we have defined $\theta_{eff}^2 = \sin^2(\theta\Delta)/\Delta^2$. If $a < (1+\Delta^2)/2$ the distribution Eq. (6) is always valid. If $\Delta = 0$ normalizability requires that $\theta^2\,(a-b) < 1$, i.e. θ must be sufficiently small if $a > 1/2$. If $\Delta \neq 0$ the mean value of photons obtained from Eq. (6) will be a periodic function of $\Delta\theta$ with a maximum $(n_b + a/\Delta^2)/(1 + (b-a)/\Delta^2)$ for $\Delta\theta = (n + 1/2)\pi$, where $n = 0, 1, \ldots$. The corresponding minimum is n_b and occurs for $\Delta\theta = n\pi$. In the thermal phase the micromaser can therefore be in a "twinkling" mode for $\Delta \neq 0$, i.e. the mean number of photons can exhibit periodic variations as a function of θ.

Non-trivial saddle-points of the effective potential $V_0(x)$, which exist only if $a > (1+\Delta^2)/2$, can be parametrically represented in the form [8]

$$\begin{aligned} x + \Delta^2 &= (a-b)\sin^2\phi \quad , \\ \theta &= \frac{1}{\sqrt{a-b}}\,\frac{\phi}{|\sin\phi|} \quad , \end{aligned} \tag{7}$$

with $\phi \geq \phi_0 \equiv \arcsin(|\Delta|/\sqrt{a-b})$. These saddle-points do not depend on n_b. If, for a given θ, there are several saddle-points, the actual maser phase is described by the saddle-point which corresponds to the global minimum of $V_0(x)$.

The first extremum of $V_0(x)$ occurs at $\theta_0^* \equiv \theta(\phi_0)$. Critical points, where new extrema of $V_0(x)$ appear, are determined by $V_0''(x) = 0$, i.e. non-trivial solutions of $\tan\phi = \phi$. Correspondning to the positive solutions $\phi = \phi_k$, where $k = 1, 2, \ldots$, we have the critical pump parameters $\theta_k = \phi_k/(|\sin\phi_k|\sqrt{a-b})$.

Using the substitution $\phi = \theta\sqrt{x+\Delta^2}$, the potential $V_0(x)$ in Eq. (4) can now be written in the form

$$V_0(\phi,\theta) = \\ -\frac{2}{\theta^2}\int_{\theta|\Delta|}^{\phi} d\phi\,\phi\,\ln[\,\frac{n_b + a\,q(\phi,\theta)}{1 + n_b + b\,q(\phi,\theta)}\,] \quad , \tag{8}$$

where $q(\phi,\theta) = \theta^2\sin^2\phi/\phi^2$. By choosing ϕ corresponding to Eq. (7) the effective potential is always at an extremum. We then get a multi-branched effective potential $V_0 = V_0(\theta)$. Branch k is swept out when ϕ varies in the range $\phi_0 + k\pi \leq \phi \leq (k+1)\pi - \phi_0$, where $k = 0, 1, 2, \ldots$. Except for the first branch ($k = 0$), each of these branches is doubled-valued. One sub-branch then corresponds to a maximum ($V_0''(x) < 0$), which is swept out first as ϕ increases, and the other corresponds to a minimum ($V_0''(x) > 0$). For a given branch k, these sub-branches coincide at the critical point θ_k (see e.g. Fig. 1).

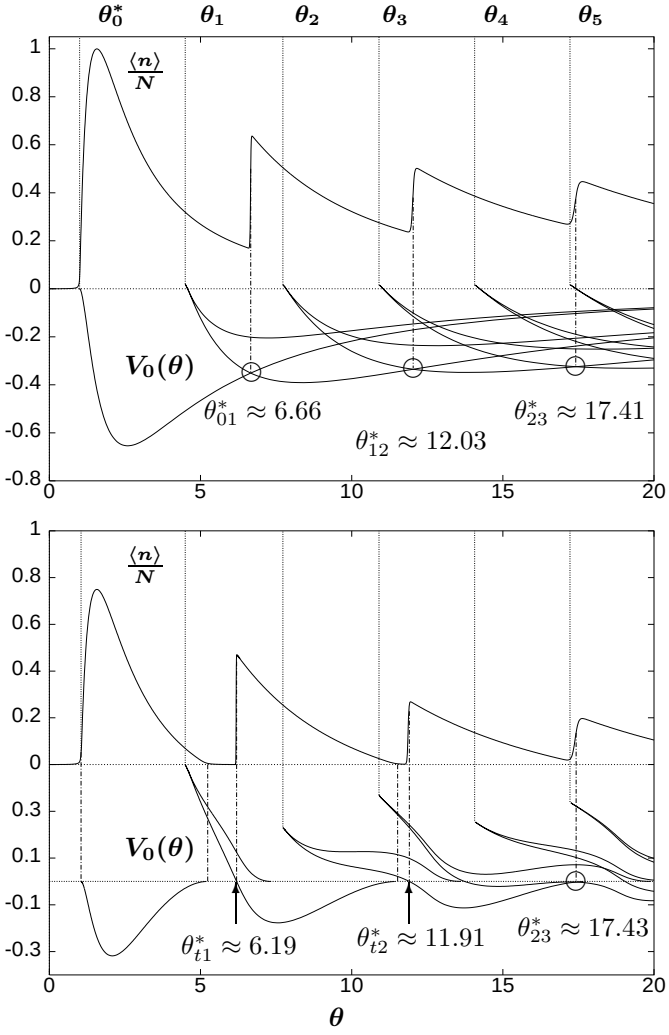

FIG. 1. The extremal values of the effective potential $V_0(\theta)$ when $a = 1$, $n_b = 0.15$, $\Delta = 0$ (upper figure) and $|\Delta| = 0.5$ (lower figure). The critical parameters θ_0^* and θ_k are shown as well as the pump parameters θ_{kk+1}^* for co-existence of two maser phases. θ_{kk+1}^*, marked by a circle, and θ_{tk}^* correspond to first-order transitions.

In Fig. 1 we illustrate such branches as well as the corresponding value of the order parameter $\langle x\rangle$. The transition from the thermal phase to the first maser phase at $\theta = \theta_0^*$ is always a second-order phase transition. The transition from one maser branch k to the neighboring maser branch $k+1$, both with $V_0''(x) > 0$, corresponds to a first-order phase transition and occurs at $\theta = \theta_{kk+1}^*$. For various k such critical points are marked by circles

in Fig. 1. As Δ increases the nature of these transitions changes. In Fig. 1 with $|\Delta| = 0.5$ the first two maser phases e.g. never intersect. Instead they intersect with the thermal phase. This phenomena corresponds to the twinkling behavior in the thermal phase even though we do not have a strictly periodic behavior. The twinkling phenomena will now, however, be more pronounced since, in the large N limit, the maser will be "dark" in the thermal phase. For $a = 1$ and $n_b = 0.15$ the phase separation of the first two maser phases occurs at $|\Delta| \approx 0.408$. With increasing value of $\Delta^2 \leq 1$ more phases are separated.

Critical transition lines can now be determined by considering intersections between the various micromaser phases. Hence, we can construct a phase diagram in e.g. the a-θ-parameter space. The result is shown in Fig. 2 for the same parameters as in Fig. 1. In the upper phase diagram in Fig. 2 the various micromaser phases are well separated, i.e. they are uniquely separated by the critical lines. The first critical line is in general determined analytically by the condition $\theta_{eff}^2\,(a-b) = 1$. The other critical lines are determined by means of analytical and numerical methods. In the lower phase diagram of Fig. 2 with $|\Delta| = 0.5$, micromaser phases which appear for sufficiently large values of θ will again be well separated.

The order parameter $\langle n\rangle/N$ can now also be studied as a function of e.g. the probability a. Fig. 3 shows such a plot. When we cross transition lines in the phase diagram the order parameter will make discrete jumps and hence also exhibits a plateau-like behavior.

Let us now consider long-time correlations in the large N limit as was first introduced in Refs. [8]. These correlations are most conveniently obtained by making use of the continuous time formulation of the micromaser system [11]. The vector p formed by the diagonal density matrix elements of the photon field then obeys the differential equation $dp/dt = -\gamma L p$, where $L = L_C - N(M-1)$. Here L_C describes the damping of the cavity , i.e.

$$(L_C)_{nm} = (n_b+1)[\,n\delta_{n,m} - (n+1)\delta_{n+1,m}\,] + n_b[\,(n+1)\delta_{n,m} - n\delta_{n,m+1}\,] \quad , \tag{9}$$

and $M = M(+) + M(-)$, where $M(+)_{nm} = bq_{n+1}\delta_{n+1,m} + a(1-q_{n+1})\delta_{n,m}$ and $M(-)_{nm} = aq_n\delta_{n,m+1} + b(1-q_n)\delta_{n,m}$ have their origin in the JC-model [6,8]. The lowest eigenvalue $\lambda_0 = 0$ of L then determines the stationary equilibrium solution $p = p^0$ as given by Eq. (1). The next non-zero eigenvalue λ of L, which we determine numerically, will then determine typical scales for the approach to the stationary situation. The joint probability for observing two atoms, with a time-delay t between them, can now be used in order to define a correlation length $\gamma^A(t)$ [8]. At large times $t \to \infty$, we define the atomic beam correlation length ξ_A by [8]

$$\gamma_A(t) \sim e^{-t/\xi_A} \quad , \tag{10}$$

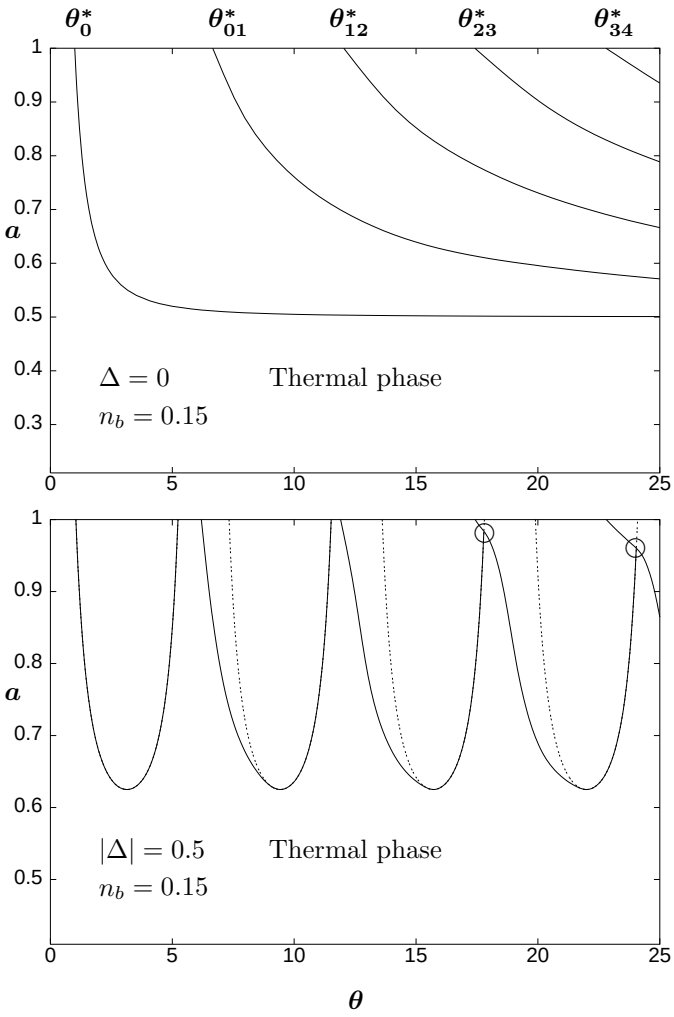

FIG. 2. Phase diagrams for the same set of parameters as in Fig. 1. The upper figure is discussed in the main text. The dashed curves in the lower figure correspond to the lines determined by $\theta_{eff}^2\,(a-b) = 1$. When not visible they overlap with the solid critical lines. The first critical line corresponds to a second-order (thermal-maser) transition. For any other critical line the transition is first-order (second-order) to the left (right) of its minimum (determined by $\sin^2(\Delta\theta) = 1$) unless it intersects with another critical line. Triple points are indicated by circles.

which then is determined by λ, i.e. $\gamma\xi_A = 1/\lambda$. For photons we define a similar correlation length ξ_C. It follows that the correlation lengths are identical, i.e. $\xi_A = \xi_C \equiv \xi$ [8]. The correlation length $\gamma\xi$ is shown in Fig. 4 for $|\Delta| = 0.5$. In the large N limit, the clear peaks in the correlation length occur at the critical pump parameters θ_0^*, θ_{tk}^* and θ_{kk+1}^*. In the thermal phase we then have $\gamma\xi \simeq 1/(1+(a-b)\theta_{eff}^2)$, provided we are not to close to a critical line. When we move from the thermal phase to a maser phase the correlation length will increase. At the critical line $(a-b)\theta_{eff}^2 = 1$, the correlation length will behave as $(\gamma\xi)_{crit} \simeq (a-b)\sqrt{N/(a+(a-b)n_b)}/2$, apart from a weak dependence of the detuning parameter Δ.

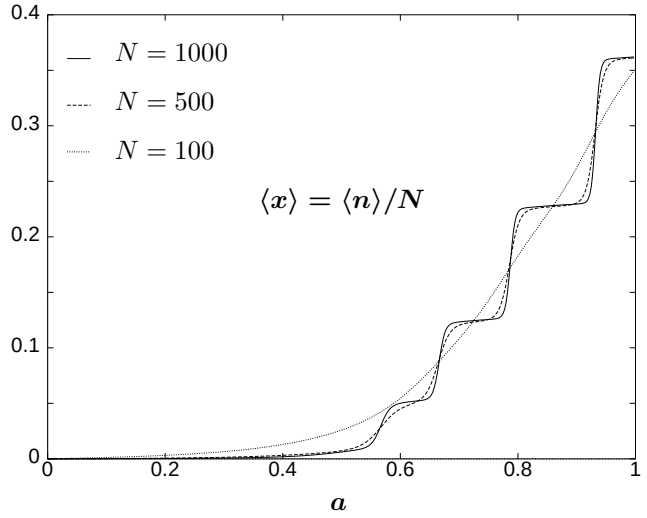

FIG. 3. Plateaus of the order parameter $\langle x \rangle = \langle n \rangle / N$ versus a when $\Delta = 0$, $n_b = 0.15$ and $\theta = 25$ for various values of N. Each step corresponds to a point on one of the transition lines in Fig. 2.

At the transition lines $\theta = \theta^*_{kk+1}$ the methods of [8] can be used to show that the correlation length depends exponentially on the combination $N(a + n_b(a - b))$. One can then also show that, as Δ^2 approaches its maximal value $a - b$ for saddle-points to exist, $\gamma\xi \to 1$ exponentially fast. In view of the recent experiments on trapping states in the stationary field configuration of the micromaser [12], we notice that high peaks occur in the atomic correlation length for such states [8]. The dependence of these trapping state peaks on the physical parameters at hand can be studied using the methods presented here.

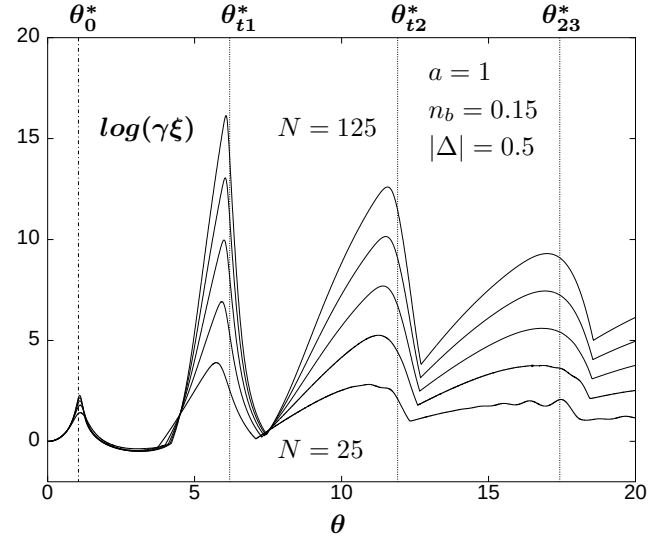

FIG. 4. The logarithm of the correlation length $\gamma\xi$ as a function of θ for various values of $N(25, 50, ...125)$. The vertical lines indicate the critical values of θ (see Fig. 1).

In conclusion we have studied, in the large N limit, the various phase transitions and critical fluctuations of the micromaser system at non-zero detuning and for pump atoms prepared in a statistical mixture. We have revealed new novel features of the system as e.g. the plateaus in the number of photons $\langle n \rangle / N$ as a function of a as well as a new twinkling mode of the micromaser system for large detuning. This twinkling phenomena has a close resemblance with the observed revivals of the micromaser system [1].

B.-S.S. wish to thank H. Walther for discussions, comments on the manuscript and for providing a guide to the experimental work. P.K.R. acknowledges support by the Research Council of Norway under the contract No. 118948/410.

[1] H. Walther, Physica Scripta **T23** (1988) 165; Phys. Rep. **219** (1992) 263; "*Experiments With Single Atoms in Cavities and Traps* " in "*Fundamental Problems in Quantum Theory* ", Eds. D. M. Greenberger and A. Zeilinger, Ann. N.Y. Acad. Sci. **755** (1995) 133; Proc. Roy. Soc. **A454** (1998) 431; Laser Physics **8** (1998) 1; Physica Scripta **T76** (1998) 138.

[2] L. Caiani, L. Casetti, C. Clementi and M. Pettini, Phys. Rev. Lett. **79** (1997) 4361; L. Casetti, E.G.D. Cohen and M. Pettini, Phys. Rev. Lett. **82** (1999) 4160.

[3] A. Buchleitner and R.N. Mantegna, Phys. Rev. Lett. **80** (1998) 3932.

[4] A. Maritan and J.R. Banavar, Phys. Rev. Lett. **72** (1994) 1451; B.-S. Skagerstam in "*Applied Field Theory* ", Eds. Choonkye Lee, Hyunsoo Min and Q-Han Park (Chungbum Publ. House, Seoul, 1999).

[5] D. Filipowicz, J. Javanainen and P. Meystre, Opt. Comm. **58** (1986) 327, Phys. Rev. **A34** (1986) 3077.

[6] E.T. Jaynes and F.W. Cummings, Proc. IEEE **51** (1963) 89.

[7] A.M. Guzman, P. Meystre and E. M. Wright, Phys. Rev. **A40** (1989) 2471.

[8] P. Elmfors, B. Lautrup and B.-S. Skagerstam, "*Correlations as a Handle on the Quantum State of the Micromaser* ", CERN/TH 95-154 (cond-mat/9506058); Physica Scripta **55** (1997) 724; Phys. Rev. **A54** (1996) 5171.

[9] O. Benson, G. Raithel and H. Walther, Phys. Rev. Lett.**72** (1994) 3506, *ibid.* **75** (1995) 3446, and "*Dynamics of the MicroMaser Field* " in "*Electron Theory and Quantum Electrodynamics: 100 Years Later* ", Ed. J.P. Dowling (Plenum Press, New York, 1997).

[10] See e.g. R. Courant and D. Hilbert, "*Methods of Mathematical Physics* " (Interscience, New York, 1953) and M. Fleischhauer and W.P. Schleich, Phys. Rev. **A47** (1993) 4258.

[11] L. Lugiato, M. Scully and H. Walther, Phys. Rev. **A36** (1987) 740.

[12] M.Weidinger, B.T.H. Varcoe, R. Heerlein and H. Walther, Phys. Rev. Lett. **82** (1999) 3795.

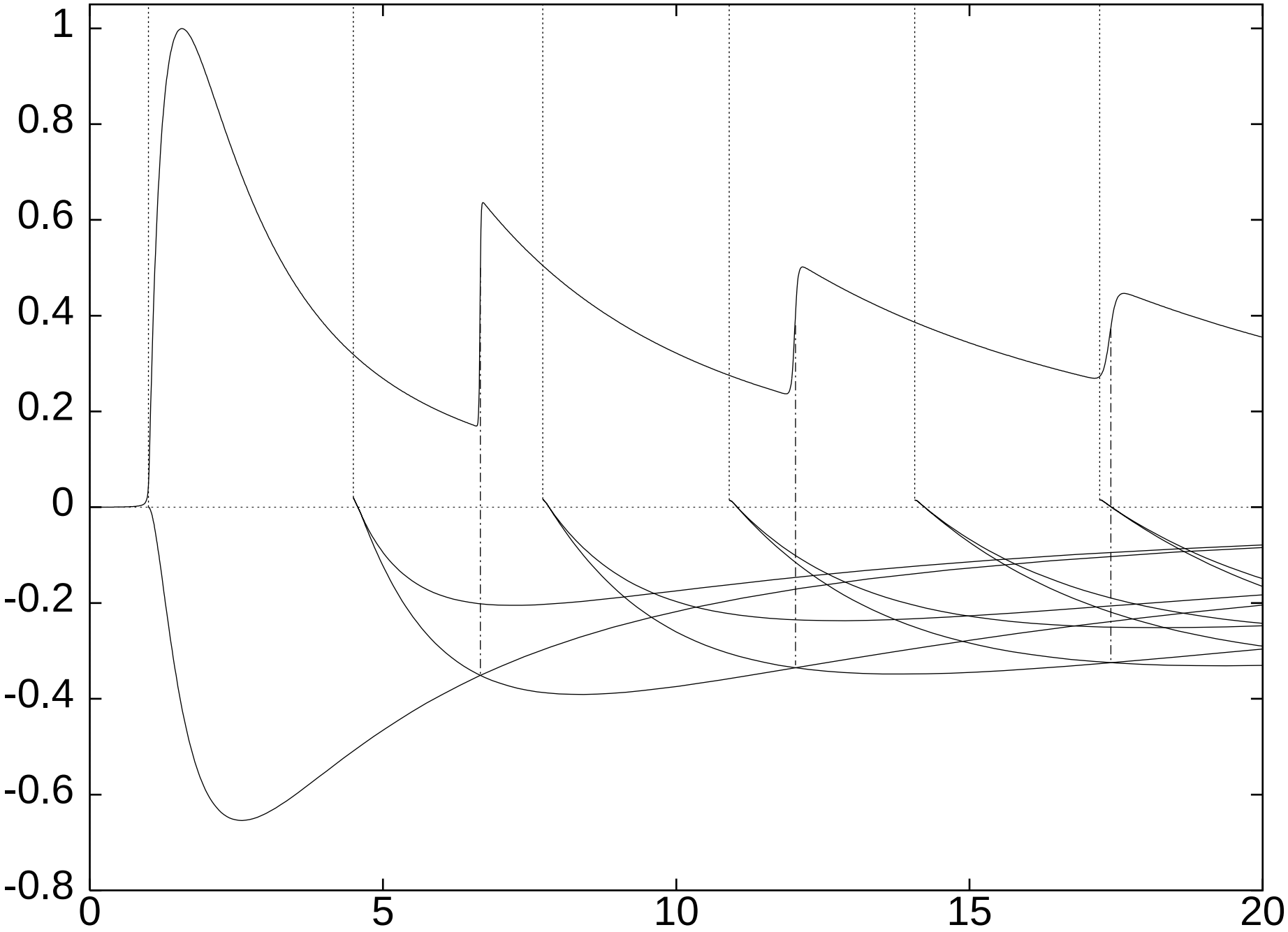
1
0.8
0.6
0.4
0.2
0
-0.2
-0.4
-0.6
-0.8
0
5
10
15
20

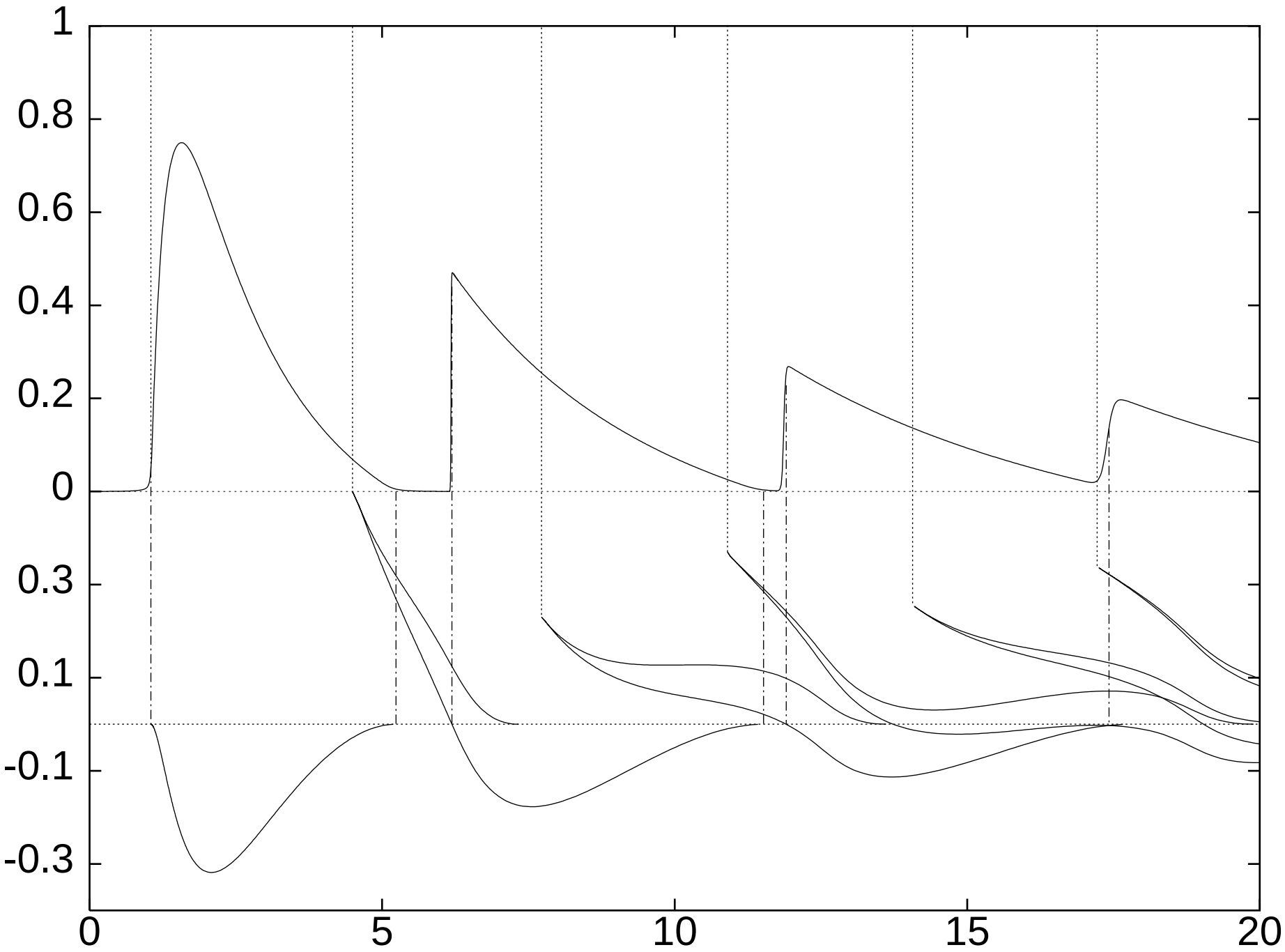
1
0.8
0.6
0.4
0.2
0
0.3
0.1
-0.1
-0.3
0
5
10
15
20

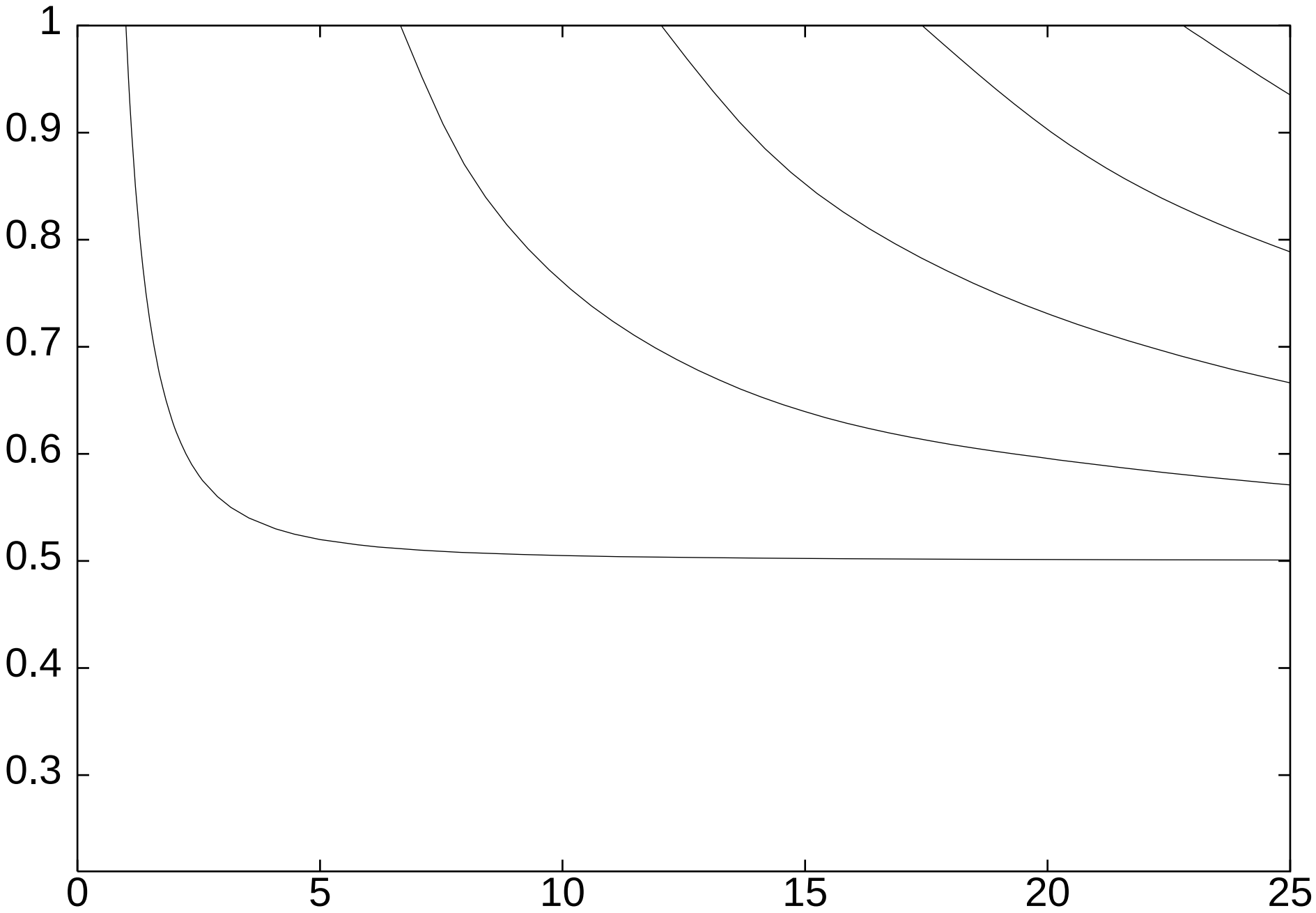
1
0.9
0.8
0.7
0.6
0.5
0.4
0.3
0
5
10
15
20
25

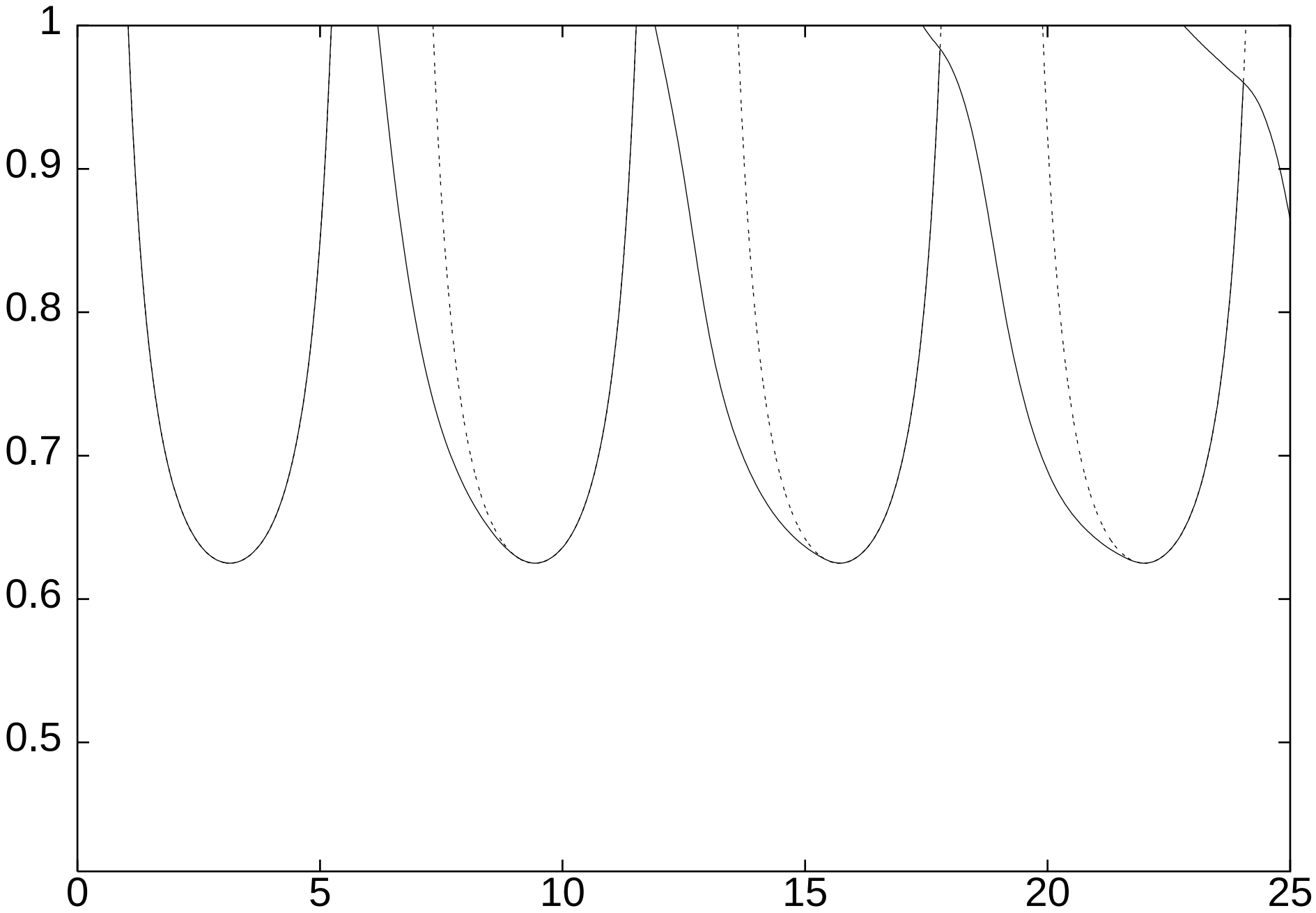
1
0.9
0.8
0.7
0.6
0.5
0
5
10
15
20
25